
# Nondestructive spectroscopic research for fast growing hybrid wood

Nagoya University
Graduate school of Bioagricultural Sciences
Department of Forest and Environmental Resources Sciences
System Engineering for Biology

Doctoral thesis

**Dang Duc Viet**

Nagoya, 2021

Table of contents

1. Introduction .....1
2. Chapter 1: Physical and mechanical properties of fast growing polyploid acacia hybrids (*A. auriculiformis* × *A. mangium*) from Vietnam .....2
2.1. Introduction .....2
2.2. Materials and Methods .....3
*2.3.1. Acacia Hybrid Polyploid Clones and Sampling* .....*3*
*2.3.2. Air-Dry Moisture Content and Basic Density* .....*3*
*2.3.3. Mechanical Testing* .....*4*
*2.3.4. Statistical Analysis* .....*4*
2.3. Results and Discussion .....4
2.4. Conclusions .....5
3. Chapter 2: Near-infrared spectroscopy and hyperspectral imaging can aid in the prediction and mapping of polyploid acacia hybrid wood properties in tree improvement programs .....6
3.1. Introduction .....6
3.2. Materials and methods .....6
*3.2.1. Acacia polyploid hybrid clones* .....*6*
*3.2.2. Material processing* .....*6*
*3.2.3. NIR measurement* .....*7*
*3.2.4. NIR hyperspectral imaging (HSI) measurements* .....*7*
*3.2.5. Partial least square (PLS) calibration* .....*7*
*3.2.6. Mapping the prediction values for the wood properties* .....*8*
3.3. Results and discussions .....8
3.4. Conclusions .....10
4. Chapter 3: Identification Acacia hybrid wood using Near-infrared hyperspectral imaging and deep learning method .....10
4.1. Introduction .....10
4.2. Methodology .....10
*4.2.1. Wood samples* .....*10*
*4.2.2. Spectral data pretreatment and NIR, HSI identification* .....*11*
*4.2.3. Construction of PC images from principal component scores* .....*11*
*4.2.4. CNN architecture for wood species identification* .....*11*
4.3. Results .....11
4.4. Conclusions .....13
5. Overview .....13
6. References .....14
7. List of publications .....16
8. List of Conferences .....16
9. Activities .....16

## 1. Introduction

Plants of the genus Acacia are an important resource in global furniture manufacturing and are vital to the wood industry of Southeast Asian countries [1–6] Improvements in technology and tree breeding techniques have increased the interest in *Acacia* products [7]. An Acacia hybrid (an interspecific hybrid of *Acacia mangium* and *Acacia auriculiformis*) was first recognized in Malaysia in 1972 [4]; since then, this hybrid has rapidly become an important tree in the industrial output of many countries, including Vietnam. Recently, *Acacia* hybrid plantation productivity and quality have been improved by using both cutting and tissue culture breeding technologies effectively in a large-scale clonal forestry. Research into, and the development of, breeding technologies has led to innovations in forestry and created cutting-edge methodologies [8], such as the breeding of polyploid *Acacia* hybrids that possess three or more sets of chromosomes [9]. This method is introducing diversity into breeding populations, reducing reproduction, fertility, and producing new wood fibers [1,10].

Nondestructive approaches such as near-infrared (NIR) spectroscopy and NIR hyperspectral images (HSI) can be employed to conduct quantitative and qualitative analysis of a specific product. Among the advantages attributed to the NIR technology, it can be highlighted the high response speed, the fact that it is a nondestructive method, with a low analytical cost per sample, with little or no need for sample preparation. Also, the same instrument is suitable for different products and analytical parameters, is not necessary the use of chemical reagents and no polluting waste is generated. These advantages and planted wood are meet the requirement for label number 3, 9, 12 and 15 in SDGs program.

NIR and HSI could be used for the assessment of wood properties in standing trees with effective costs [11,12]. These previous investigations indicate that wood property variations, both within and between trees, have not yet been fully described. Moreover, the performance of the NIR and HSI on *Acacia* wood properties for whole trees, both within and between clones, is limited. Hence, there is a need to estimate whole tree and between tree properties for tree improvement programs, and to evaluate how NIR and HSI could be utilized for this determination.

Wood species identification is important because validation of the correct species is a key factor for confirming wood properties and estimating wood products price.

Moreover, wood species discriminant is always accomplished by skilled personnel with comprehensive knowledge of wood anatomy. Several analytical techniques, such as those based on microscopic features, DNA barcoding technology have been applied in identification. However, those methods are mostly destructive and require specialized skill, which can be time-consuming. NIR, HSI combine with deep learning have also been used for discrimination between different species. These techniques have been attracting attention recently and achieved high accuracy in various recognition tasks.

The purpose of this study was to evaluate *Acacia* wood properties using traditional method and non-destructive method by NIR spectroscopy and hyper spectral imaging. The wood species identification by NIR, HSI combine deep learning was the second purpose. To achieve the goal, totally three research topics were done in this PhD course:

1. The physical and mechanical properties including moisture content, basic density, modulus of rupture, modulus of elasticity and Young's modulus of nine *Acacia* clones were measured by traditional method follow ISO standards.

2. Then the models and mapping results by NIR and HSI were created to predict wood properties.

3. The wood species was identified following NIR, HSI data and deep learning technique.

Each topic will be presented and discussed separately in this thesis:

## 2. Chapter 1: Physical and mechanical properties of fast growing polyploid acacia hybrids (*A. auriculiformis* × *A. mangium*) from Vietnam

### 2.1. Introduction

Many studies on this *Acacia* hybrid, aimed at providing information for end-use applications, have shown that it is fast growing, has a medium strength, and can be utilized in many ways. The *Acacia* hybrid has also been shown to meet the requirements for use as pulp, use in the paper industry, and for certain various uses such as tool handles, furniture, and pallets [13].

Although some research on the properties of polyploid *Acacia* hybrids has been conducted, there is currently a limited understanding of the various wood properties of the clones. Therefore, in the present study, we investigated the physical and mechanical properties of the wood from polyploid *Acacia* hybrid clones from Vietnam. The

relationships among the wood properties and clones were also evaluated, with the aim of improving breeding programs.

## 2.2. Materials and Methods

### *2.3.1. Acacia Hybrid Polyploid Clones and Sampling*

The materials used in this study were collected from seven *Acacia* hybrid clonal trials established by the Institute for Forest Tree Improvement and Biotechnology (Vietnamese Academy of Forest Sciences), between 2014 and 2018. The trial sites are located in Dong Nai (10°57’ N, 106°49’ E) in southern Vietnam. The soil type in the site is sandy alluvium, the mean annual rainfall is 1640 mm, and the mean annual temperature is 27 °C.

*Acacia* hybrid diploid (2×) clones available for commercial breeding, namely BV10 and BV16, were chosen as control clones. The best selection of commercial *Acacia* hybrids were transformed into tetraploid (4×) clones by in vitro colchicine treatment. Triploid (3×) clones could then be produced by pollination between 2× and 4×. Five ramets of each of the four 2× and 3× clones (i.e., BV10, BV16, X101, and X102), together with three 4× trees of tetraploid taxa (i.e., *A. auriculiformis*, *A. mangium*, and the *Acacia* hybrid) were felled at age 3.8 years to collect wood samples.

Logs that were 0.2–1.3 m and 1.5–3 m in length were taken from each tree stem after felling, to extract samples for measurement of mechanical properties. 5-cm disks were also taken to test physical properties at various height levels (0.2–13.5 m). Disk edges were coated with wax to prevent decay and other environmental alterations. DBH (1.3 m) was determined as the mean of two cross diameters. After felling, total height was also measured.

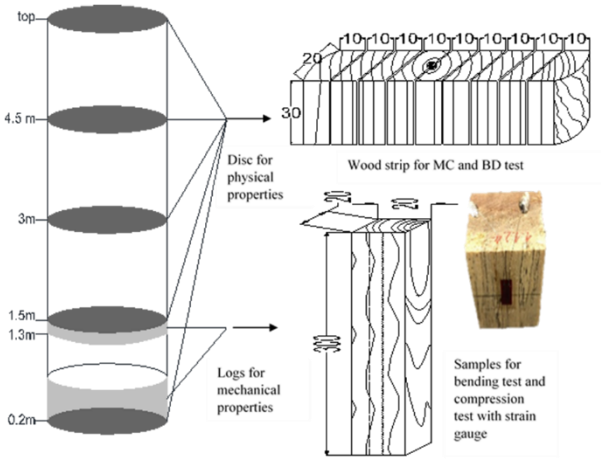


**Figure 2.1.** Sampling methods for discs and logs and test samples for physical and mechanical properties. (MC, moisture content; BD, basic density)

### *2.3.2. Air-Dry Moisture Content and Basic Density*

Pith-to-bark strips (diameter × 30 × 20 mm) were cut from each disk after air drying. The strips were then divided into small pieces at a distance of 1 cm from pith-to-bark with a razor blade. Each piece was weighed at the air-dry stage and then dried

at 103°C ± 3°C to determine dry weight. Equilibrium air-dry moisture content was determined at room temperature (around 25°C) and humidity (25%–35% relative humidity (RH)). Basic density was measured with an electronic densimeter (EW-300SG, Alpha Mirage, Osaka, Japan).

*2.3.3. Mechanical Testing*

Specimens for static bending (20 × 20 × 320 mm, radial × tangential × axial) and compression (20 × 20 × 30 mm, radial × tangential × axial) were cut from a 20-mm-thick board. The specimens were conditioned to a constant mass at 20 °C ± 2 °C and a RH of 65% ± 5%. They were then maintained in this condition until required for testing. The average moisture content of the test samples at this stage was 12%. The modulus of rupture (MOR) and modulus of elasticity (MOE) were determined by a three-point bending test according to ISO 13061–3:2014 and ISO 13061–4:2014 standards [14,15]. After these tests were completed, samples were taken from undamaged portions to determine density for estimating the relationship between bending and density.

Compression parallel to the grain was performed in a 100 kN universal testing machine (AG-I, Shimazdu, Japan). The displacement was measured using strain gage (FLAB 511, TML, Japan) with a gage factor of 2.1% ± 1%. Compression strength and Young's modulus (YM) were determined according to ISO 13061–17:2017 and ISO 130614:2014 standards [15,16].

*2.3.4. Statistical Analysis*

The statistical analysis involved a completely randomized design. ANOVA was used to test for differences in the outcomes of experiments with different numbers of samples. Averages were compared using Tukey's test. The Mann–Whitney U test was also used to test for differences between clone in terms of their physical and mechanical properties. The significance level in all tests was $p < 0.05$.

**2.3. Results and Discussion**

As presented in Table 2.1, the mean moisture contents of the seven clones were significantly different. Moreover, the data could be divided into two groups: the 4x genotypes in one group and the other clones in a second group. Because wood is always exposed to varying climatic conditions, defining the equilibrium moisture content (EMC) is important for the effective use of wood. Mechanical properties and shrinkage changes, which are probably the most important issues in the end-use applications of

solid wood, are positively correlated with the EMC of wood [17–19]. The wood properties are related to heartwood and sap wood ratio, where the heartwood absorbs less water than sapwood [20–25]. This is same tendency with changing in EMC, which is affected by heartwood to sapwood ratio [26] as well as wood density [24,25].As shown in Table 2.1, the basic densities of AA-4× and AM-4× were significantly different from those of BV10 and BV16; however, the basic densities of X101, X102, and AH-4× did not differ from those of BV10 and BV16.

The Table 2.1 showed a significant difference between the MOR of X101 and AM-4× and those of the control clones BV10 and BV16. There was a significant difference in the stress value between AM-4× and the control clones. Likewise, the Young's modulus of AM-4× was significantly lower than that of the diploid group, whereas that of AH-4× was considerably higher than the values of the control group. This result suggests that other triploid and the tetraploid clones have similar compression strengths to the control.

**Table 2.1.** Wood properties and ANOVA results in different clones.

| | MC (%) | BD (g/cm$^3$) | MOR (MPa) | MOE (GPa) | σ (N/mm$^2$) | E (GPa) |
|---|---|---|---|---|---|---|
| BV10 | 5.1 c<br>(0.2) | 0.47 b<br>(0.06) | 71 ab<br>(17) | 8.7 bc<br>(1.1) | 46.0 a<br>(6.7) | 9.6 bc<br>(1.3) |
| BV16 | 5.1 c<br>(0.3) | 0.44 cd<br>(0.07) | 75 ab<br>(15) | 8.6 bc<br>(0.8) | 44.6 a<br>(5.4) | 9.2 c<br>(1.5) |
| X101 | 5.4 b<br>(0.3) | 0.45 c<br>(0.07) | 79 a<br>(14) | 9.7 a<br>(1.2) | 45.3 a<br>(5.5) | 9.9 ab<br>(1.3) |
| X102 | 5.9 a<br>(0.4) | 0.43 d<br>(0.07) | 70 b<br>(12) | 8.5 bc<br>(1.3) | 44.4 a<br>(5.8) | 9.3 c<br>(1.3) |
| AA-4x | 4.5 d<br>(0.2) | 0.50 a<br>(0.05) | 72 ab<br>(11) | 8.2 c<br>(1.2) | 44.0 a<br>(6.0) | 8.9 cd<br>(1.7) |
| AM-4x | 4.6 d<br>(0.4) | 0.37 e<br>(0.10) | 56 c<br>(11) | 7.2 d<br>(0.9) | 38.1 b<br>(5.6) | 8.2 d<br>(1.3) |
| AH-4x | 4.6 d<br>(0.3) | 0.42 d<br>(0.06) | 71 ab<br>(11) | 9.2 ab<br>(0.9) | 46.5 a<br>(3.8) | 10.3 a<br>(1.0) |

Data are show as mean with different group in letters; values in parentheses represent for standard deviation. MC, moisture content; BD, basic density; MOR, module of rupture; MOE, module of elasticity; σ, ultimate stress in compression parallel to the grain; E, Young's modulus in compression parallel to the grain.

## 2.4. Conclusions

Various clones had various advantages and disadvantages in this study. For example, AA-4× had significantly higher wood density than the other clones, while AM-4× had greater stem volume than the control clones. In addition, X101 had higher stem volume and bending properties (MOR and MOE) than the other clones, and similar wood density to the control. In general, triploid and tetraploid *Acacia* hybrids have the potential to be alternative species to supply *Acacia* wood as valuable hardwood timber.

Moreover, X101 could potentially be used for selection to improve and increase the production of high-quality *Acacia* wood.

## 3. Chapter 2: Near-infrared spectroscopy and hyperspectral imaging can aid in the prediction and mapping of polyploid acacia hybrid wood properties in tree improvement programs

### 3.1. Introduction

The performance of the NIR and HSI on *Acacia* wood properties for whole trees, both within and between clones, is limited. Hence, there is a need to estimate whole tree and between tree properties for tree improvement programs, and to evaluate how NIR and HSI could be utilized for this purpose. The aims of this investigation were to: (1) predict physical and mechanical properties using NIR and HSI for polyploid *Acacia* hybrid wood collected from Vietnam; and (2) map wood properties to examine how specific gravity (SG) and air-dry equilibrium moisture content (MC) changed both between and within clones.

### 3.2. Materials and methods

#### *3.2.1. Acacia polyploid hybrid clones*

Nine Acacia hybrid clones from a plantation at the Institute for Forest Tree Improvement and Biotechnology, Dong Nai, Vietnam were selected for this study. Acacia hybrid diploid (2×) clones from commercial breeding, namely BV10, BV16, and AH-2× were chosen. The tetraploid (4×) clones were transformed from the best diploid clone using in vitro colchicine treatment and those selected included *Acacia auriculiformis* (AA-4×), *Acacia mangium* (AM-4×), and the *Acacia* hybrid (AH-4×). Triploid (3×) clones produced via pollination between 2× and 4× included X101, X102, and X41. The sample trees were felled at 3.8 years of age, except for AH-2×, which was felled at 8 years of age. Five ramets of each of the 2× and 3× clones together with three 4× trees were collected for sample.

#### *3.2.2. Material processing*

Logs that were 0.2–1.3 m and 1.5–3 m in length were taken from each tree stem after felling to use as the bending and compression test samples. Samples from the five AH-2× trees were taken when they were 1.3 m in height to compare their properties with the other clones in the mapping results. 5-cm disks were taken at various heights (0.2–

13.5 m) for the MC and SG measurements of the specimens. The sampling processes were previously described in 2.3.1.

*3.2.3. NIR measurement*

The FT-NIR spectrometer was a Matrix-F (Bruker Optics GmbH) with a wavenumber range of between 10,000 $cm^{-1}$ and 4000 $cm^{-1}$ (wavelengths: 1000–2500 nm) and a resolution of 4 $cm^{-1}$ working in diffuse absorbance mode. Spectra were collected from: three positions nearly in the center of the cross section of the MC and SG samples; three positions on each face of the two tangential/longitudinal sides of the bending samples, in which one side was in contact with the pressure beam directly during the bending test and the other was on the opposite side; four positions in the four tangential sections of the compression samples, of which two were attached with strain gages in the compression test. 32 scans were collected for each position and all the scans were averaged into a single spectrum.

*3.2.4. NIR hyperspectral imaging (HSI) measurements*

The hyperspectral imaging device (Compovision; Sumitomo Electric Industries, Ltd., Tokyo, Japan) used a push broom line scanning system that covered the spectral range from 913 to 2518 nm in 256 spectral bands (spectral resolution of 6.2 nm) with 320 × 533 spatial pixels. Before collecting the sample images, a white plate was placed at the same position as the sample with the same parameters and used as a reference ($W$). The dark current ($D$) was obtained by turning the light source off and fully covering the lens with its cap. The relative reflectance ($R$) of all collected spectral images was then calculated using the measured images ($I$), in accordance with the following formula:

$$R = \frac{I - D}{W - D} \qquad (Eq. 3.1)$$

*3.2.5. Partial least square (PLS) calibration*

The spectral data from all samples were split randomly into the calibration and prediction sets, which consisted of 70% for calibration and 30% for prediction. MATLAB was used for data processing and image analysis. The PLS models were developed for a spectral range of 1000–2500 nm for the NIR and 1033 to 2230 nm for the HSI. Raw spectra were pre-processed with the SNV and 2$^{nd}$ derivative (SP2D). These techniques were applied because they could reduce physical interference while maintaining the chemical information [27]. Determination coefficients for cross

validation ($R^2$), the root mean square error of cross-validation (RMSECV) and the root mean square error of prediction (RMSEP) were calculated. The maximum number of latent variables (LV) was fixed at five for SG and MC and ten for the other properties.

*3.2.6. Mapping the prediction values for the wood properties*

The best calibration model for the PLS analyses resulted from the HSI spectra with the pre-processing treatment (SP2D by segment (s) = 3 and gap (g) = 0 combined SNV in 5 LVs for SG, MC and 10 LVs for mechanical properties) was performed by mapping the wood properties.

The images of the mapped bending and compression prediction values were compared for two types of values (the lowest and the highest) to observe the variation distributions of the mapped prediction values on the sample surfaces. The HSI data spectra for the SG and MC were mapped for all the samples from the pith to bark and constructed into each clone from the butt-end to top of the tree. These maps described the distribution of the SG and MC predicted values for the whole sample within and between the clones.

### 3.3. Results and discussions

**PLS calibration**

For SG and MC, 5 factors were chosen for both the NIR model and the HSI model resulting in an $R^2$ of 0.59 and 0.85 for the SG and MC of NIR, 0.49 and 0.62 for the SG and MC of HSI, respectively. The RMSECV of the SG for NIR and HSI were 0.06 ($g/cm^3$), while the MC for NIR and HSI were 0.22 (%) and 0.16 (%), respectively.

When NIR was used to predict MOR, an $R^2$ of 0.30 and RMSECV of 12.4 (MPa) were obtained at 9 LV. Similarly, when predicting MOR by HSI, $R^2$ of 0.32 and RMSECV of 12.2 (MPa) were obtained at 10 LV. For NIR and HSI, the calibration model for MOE gave an $R^2$ of 0.65 and 0.66 respectively, and RMSECV of 0.9 (GPa). The prediction using NIR for Young's modulus was slightly weaker than that of HSI as there was an $R^2$ of 0.22 compared to 0.30, respectively, with the RMSECV of 1.29 (GPa) and 1.22 (GPa). For Young's modulus prediction, 7 LV was chosen for the NIR and 10 LV HSI models.

**Mapping for MOR, MOE, and compression**

The mapped MOR, MOE, and compression prediction data were constructed for the low and high reference data in Figure 3.2. The higher reference values are well reflected by the higher mapping results. The significant differences in the color map can clearly be seen when comparing the low and high reference values. We expected that the results of the mechanical property mapping in this study may reveal some useful information affecting wood factors, such as defects, position in the heartwood, and sapwood to mechanical properties. However, as the samples in this study are hardwood species, the difference in strength at the different positions around the earlywood and latewood are small. Thus, the mapping results here only show the differences between the low and high values of the mechanical properties.

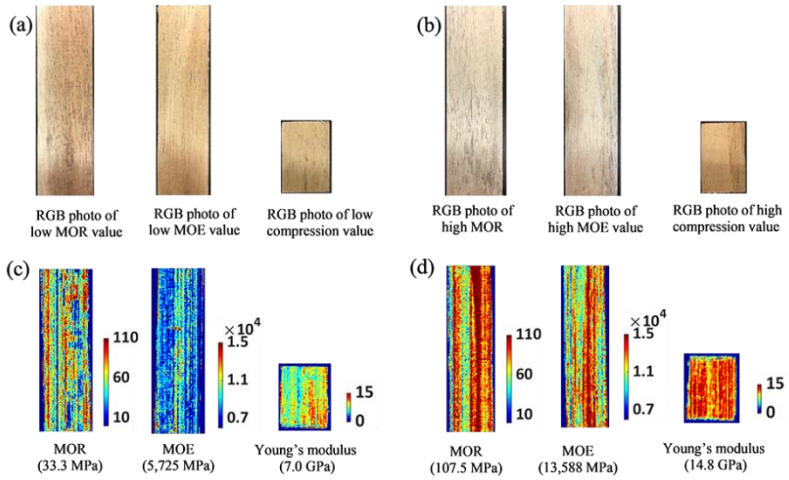


**Figure 3.2.** RGB photos (a, b) and mapping level of low and high wood properties prediction values for MOR, MOE and Young's modulus (c, d); values in parentheses represent for reference values

**Mapping within and between tree variations for SG and MC**

The SG was described in different clones and different heights of trees (Figure 3.3). In each tree, the SG was lower in the area near the pith, while it is higher on the bark side. From the end-butt logs to top, SG showed a decreasing tendency. Five disks at 1.3 m in AH-2× in doubles age older than the other clones had the same trend from the pith to bark. This proved that the age of the trees was not largely affected by the tendencies of the SG distributions. Nevertheless, this inclination was not clear in the AA4× clone. The SG mapping was expanded and corroborated the work of Viet et al. (2020).

The lower MC tended to be located nearer the pith side. The prediction of the AA4× mapping results replicated this trend. The MC values for the five AH-2× trees were similar between themselves but lower when compared to the other clones. These results determined that the MC is more dependent on the internal properties than the ambient conditions that were examined using the NIR-HSI method. Previous research

that studied the effects of the extractives and the relationships between the heartwood-sapwood and wood moisture content may not explain this result [17,24,26,29,30]. However, the MC and SG mapping may explain that those properties depend on tree diameter rather than cambial age. This finding is strong consistent with result for *Acacia* in a study which described by Kojima et al. (2009) [31].

### 3.4. Conclusions

NIR had a better performance in the prediction of physical properties than of HSI but HSI could identify the variations in the wood properties better than NIR. The SG, MC, and MOE were acceptably predicted by NIR and HSI but the MOR and Young's modulus had low predictions. All wood properties were mapped well by the HSI instrument. The variations in SG and MC for the whole trees and between the trees was well reflected by the HSI mapping. The SG and MC mapping results described the relationship between their value and sample positions in the tree.

## 4. Chapter 3: Identification Acacia hybrid wood using Near-infrared hyperspectral imaging and deep learning method

### 4.1. Introduction

In this chapter, we used HSI spectra which obtained from SG, MC samples in chapter 2 to identify 9 clones of *Acacia* wood. The principal component analysis (PCA) was applied in classification method. Then, we apply convolutional neural networks (CNN) to HSI data to construct a protocol that can automatically identify 1187 samples into 9 species with a nondestructive and rapid manner. The pre-treatments were SNV and SP2D. Subsequently, the light absorption features of each sample (HSI data) were compressed into PC scores in order to facilitate the analysis of deep learning. Finally, CNN (deep learning) prediction models based on PC images from HSI spectra were built and compared with identification results using HSI with the same pre-treatments.

### 4.2. Methodology

#### *4.2.1. Wood samples*

The samples were taken from SG, MC samples which examined in chapter 2. The total number of samples was 1187. Each sample was approximately 10 mm (radial) × 30 × 20 mm. Size differences among the samples did not affect our final results because hyperspectral images were cut to the same dimensions (217 × 186 pixel) for deep learning.

*4.2.2. Spectral data pretreatment and NIR, HSI identification*

The HSI spectral from samples which acquired from SG, MC samples in chapter 2 were used in this study. The HSI spectral range of 1033–2230 nm was selected for further data analysis because the other ranges were found to be noisy. The reflectance HSI images (217 × 186 pixel) of each sample were taken from whole spectral cube. SNV and SP2D (s=3, g=0) spectral pretreatment was used for HSI pre-treatment. Then HSI average spectral were used to identify using support vector machine (SVM) and PCA with 6 principal components (PC). The samples were randomly selected with ratio 70% for calibration set and 30% for test set in the model.

*4.2.3. Construction of PC images from principal component scores*

SNV and SP2D preprocessed spectra in training subset were averaged over the entire surface of the samples. The loading matrix was calculated from the averaged spectra. The optimal number of principal components was determined on the condition that the explanatory variance increased significantly. This calculation was performed by the leave-one-out cross-validation method. PC images (score matrix) were constructed based on the loading matrix and SNV, SP2D pretreated reflectance images in each subset. Next, the PC images were standardized by mean-value and standard deviation of each PCs in training subset.

*4.2.4. CNN architecture for wood species identification*

The model was developed on a Google Colaboratory with Intel(R) Xeon(R) 2.30 GHz CPU and NVIDIA Tesla K80 GPU. The code was written using TensorFlow & Keras in open-source python library for machine learning. Data enter neural networks through input layers including the size of images and the number of color channels. Convolutional layer convolves the input image with a set of learnable filters, with each output image having one feature map. Rectified Linear Unit (ReLU) function was used as the activation function in the convolutional layers and the fully connected layers. In the output layer, the Softmax function maps the non-normalized output to a probability distribution over predicted output classes.

**4.3. Results**

The confusion matrix of HSI and deep learning classification for test set results were presented in Figure 4.1 and 4.2. The accuracy for HSI identification was inferior to that of HSI with 85% and 91% respectively. The result could indicate the robustness

of the constructed SVM classification model. The result also shows that deep learning could improve the accuracy of wood identification.

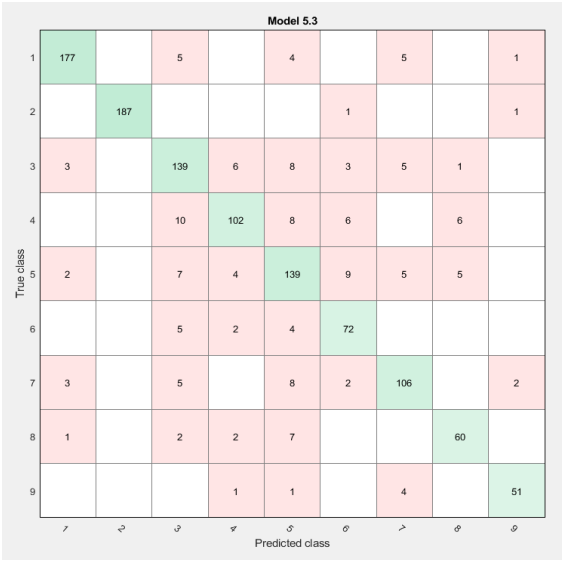


Figure 4.1. Confusion matrix for the HSI classification result

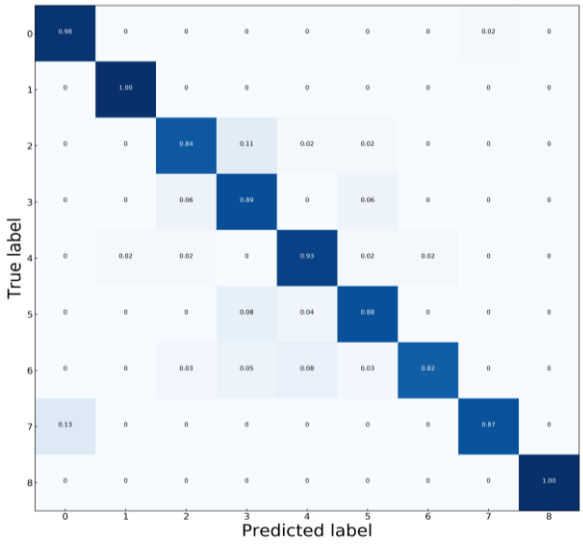


Figure 4.2. Confusion matrix for the deep learning classification result

Figure 4.3 shows the PCA loading for HSI spectral at 6 PC. PC6 loading was responsible for explaining the cellulose absorption and water absorption. Scatter plot in Figure 4.4. may explain how the HSI can identify 9 clone species. Several aspects of molecular vibration and rotation shown as reflectance spectra were efficiently expressed as PC. Also, the results from chapter 1 revealed that density and moisture content of 9 clone was significantly different.

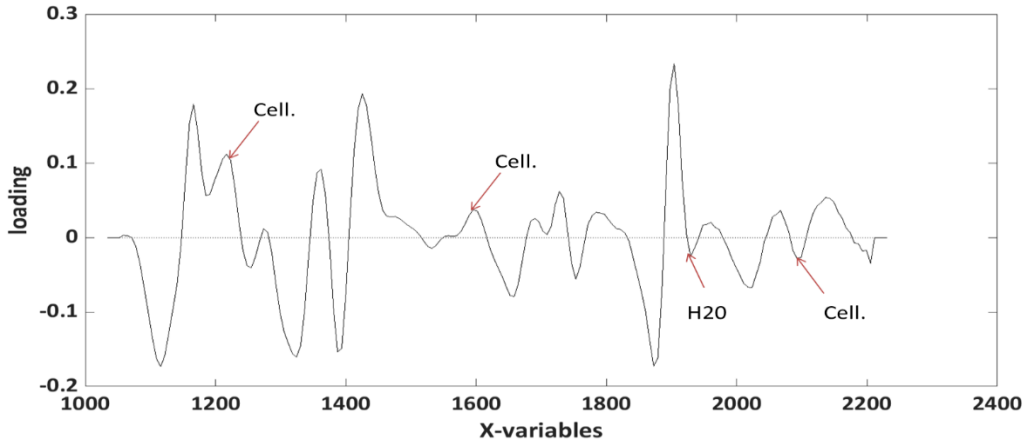


Figure 4.3. PCA loading for HSI spectral at 6 PC

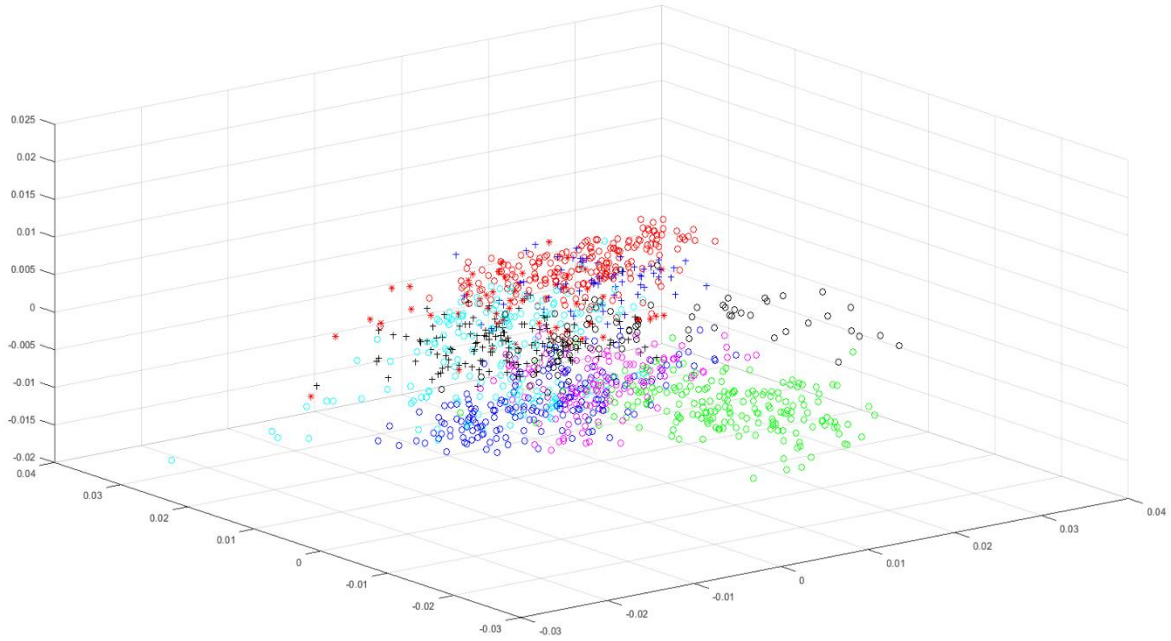


Figure 4.4. Scatter plot for PC4-PC3-PC5

## 4.4. Conclusions

In this chapter, HSI combined with the CNN approach was evaluated for 9 wood species identification. Deep learning results demonstrated that the accuracy of species identification based on HSI was 84%, and this improved to 91% using 6PC images obtained from NIR hyperspectral images.

Deep learning proved to be useful for wood analysis from the ground that the HSI via PCs efficiently expressed molecular information and contribute to better prediction than the result of using only HSI.

# 5. Overview

Considering wood density, strength, and compression properties will be important for the improvement of the polyploid *Acacia* breeding program. Our results suggest that polyploid *Acacia* hybrids have the potential to be alternative species for providing wood with improved properties to the forestry sector of Vietnam. Furthermore, the significant differences among the clones indicate that opportunities exist for selection and improvement of wood quality via selective breeding for specific properties.

The application of NIR and HSI spectroscopy was well accomplished the assessment in *Acacia* wood properties as well as identify the wood species. The NIR predicted wood physical properties better than HSI, while they provided similar predictions for the mechanical properties. The mapping results showed low densities

around the pith area and high densities near the bark. They also revealed that the EMC changed at different positions within a disk and was dependent on its position within the tree. Overall, NIR and HSI were found to be potential wood property prediction tools, suitable for use in tree improvement programs.

## 6. References


1. Griffin, A.R.; Chi, N.Q.; Harbard, J.L.; Son, D.H.; Harwood, C.E.; Price, A.; Vuong, T.D.; Koutoulis, A.; Thinh, H.H. Breeding polyploid varieties of tropical acacias: progress and prospects. *South. For.* **2015**, *77*, 41–50.
2. Griffin, A.R.; Nambiar, E.S.; Harwood, C.E.; See, L.S. Sustaining the future of Acacia plantation forestry – a synopsis. *South. For.* **2015**, *77*, v–viii.
3. Nambiar, E.S.; Harwood, C.E.; Kien, N.D. Acacia plantations in Vietnam: research and knowledge application to secure a sustainable future. *South. For.* **2015**, *77*, 1–10.
4. Pinso, C.; Nasit, R. The Potential Use of Acacia mangium x Acacia auriculiformis Hybrid in Sabah. In Proceedings of the Breeding Technologies for Tropical Acacias; 1991; Vol. 37, pp. 101–109 132.
5. Turnbull, J.W.; Midgley, S.J.; Cossalter, C. Tropical acacias planted in Asia: an overview. In Proceedings of the Recent developments in acacia planting: proceedings of an international workshop held in Hanoi, Vietnam, 27 - 30 October 1997; pp. 14–28.
6. Bueren, M. Van *Acacia Hybrids in Vietnam*; Impact Assessment Serie Report; Canberra, Australia, 2004;.
7. Nirsatmanto, A.; Sunarti, S.; Praptoyo, H. Wood Anatomical Structures of Tropical Acacias and its Implication to Tree Breeding. *Int. J. For. Hortic.* **2017**, *3*, 9–16.
8. Kha, L.D.; Ha, H.T. Research and development of acacia hybrids for commercial planting in Vietnam. *Vietnam J. Sci. Technol. Eng.* **2017**, *59*, 36–42.
9. Ramsey, J.; Schemske, D.W. Pathways, mechanisms, and rates of polyploid formation in flowering plants. *Annu. Rev. Ecol. Syst.* **1998**, *29*, 467–501.
10. Quynh Nghiem, C.; A. Griffin, R.; L. Harbard, J.; Harwood, C.E.; Le, S.; Duc Nguyen, K.; Van Pham, B. Reduced fertility in triploids of Acacia auriculiformis and its hybrid with A. mangium. *Euphytica* **2018**, *214*.
11. Meder, R. The magnitude of tree breeding and the role of near infrared spectroscopy. *NIR news* **2015**, *26*, 8–10.
12. Schimleck, L.; Dahlen, J.; Apiolaza, L.A.; Downes, G.; Emms, G.; Evans, R.; Moore, J.; Pâques, L.; Van den Bulcke, J.; Wang, X. Non-destructive evaluation techniques and what they tell us about wood property variation. *Forests* **2019**, *10*.
13. Sharma, S.K.; Shukla, S.R.; Sujatha, M. Physical and mechanical evaluation of 8-years-old acacia hybrid (a. mangium x a. auriculiformis) clones for various end uses. *Indones. J. For. Res.* **2018**, *5*, 95–102.
14. ISO 13061-3 Physical and mechanical properties of wood - Test methods for small clear wood specimens - Part 3: Determination of ultimate strength in static bending. *Geneva - Switz.* 2014.
15. ISO 13061-4 Physical and mechanical properties of wood - Test methods for small

clear wood specimens - Part 4: Determination of modulus of elasticity in static bending. *Geneva - Switz.* 2014.
16. ISO 13061-17 Physical and mechanical properties of wood - Test methods for small clear wood specimens - Part 17: Determination of ultimate stress in compression parallel to grain. *Geneva - Switz.* 2017.
17. Hernández, R.E. Moisture sorption properties of hardwoods as affected by their extraneous substances, wood density, and interlocked grain. *Wood Fiber Sci.* **2007**, *39*, 132–145.
18. Mottonen, V.; Herajarvi, H.; Koivunen, H.; Lindblad, J. Influence of felling season, drying method and within-tree location on the brinell hardness and equilibrium moisture content of wood from 27–35-year-old Betula pendula. *Scand. J. For. Res.* **2004**, *19*, 241–249.
19. Peng, H.; Jiang, J.; Zhan, T.; Lu, J. Influence of Density and Equilibrium Moisture Content on the Hardness Anisotropy of Wood. *For. Prod. J.* **2016**, *66*, 443–452.
20. Metsa-Kortelainen, S.; Antikainen, T.; Viitaniemi, P. The water absorption of sapwood and heartwood of Scots pine and Norway spruce heat-treated at 170 ◦C , 190 ◦C , 210 ◦C and 230 ◦C. *Holz als Roh - und Werkst.* **2006**, *64*, 192–197.
21. Sjökvist, T.; Blom, Å. The influence of coating color, heartwood and sapwood, on moisture content and growth of microorganisms on the surface during outdoor exposure of Norway spruce boards. *J. Coatings Technol. Res.* **2019**.
22. Sjökvist, T.; Wålinder, M.E..; Blom, Å. Liquid sorption characterisation of Norway spruce heartwood and sapwood using a multicycle Wilhelmy plate method. *Int. Wood Prod. J.* **2018**, 1–8.
23. Fredriksson, M.; Lindgren, O. End grain water absorption and redistribution in slow-grown and fast-grown Norway spruce (Picea abies ( L.) Karst.) heartwood and sapwood. *Wood Mater. Sci. Eng.* **2013**, *8*, 242–252.
24. Sivertsen, M.S.; Vestøl, G.I. Liquid water absorption in uncoated Norway spruce (Picea abies) claddings as affected by origin and wood properties. *Wood Mater. Sci. Eng.* **2010**, *5*, 181–193.
25. Sjökvist, T.; Blom, Å.; Wålinder, M.E.. The influence of heartwood , sapwood and density on moisture fluctuations and crack formations of coated Norway spruce in outdoor exposure. *J. Wood Sci.* **2019**, *65*.
26. Ball, R.D.; Simpson, I.G.; Pang, S. Measurement, modelling and prediction of equilibrium moisture content in Pinus radiata heartwood and sapwood. *Holz als Roh - und Werkst.* **2001**, *59*, 457–462.
27. Goyaghaj, A.H. Using hyperspectral images to map moisture content and basic density of boards and frozen and thawed logs, Ph.D. thesis., University of New Brunswick, Canada, 2009.
28. Viet, D.D.; Ma, T.; Inagaki, T.; Kim, N.T.; Chi, N.Q.; Tsuchikawa, S. Physical and mechanical properties of fast growing polyploid acacia hybrids (A. auriculiformis x A. mangium) from Vietnam. *Forests* **2020**, *11*, 1–15.
29. Jankowska, A.; Drozdzek, M.; Sarnowski, P.; Horodenski, J. Effect of extractives on the equilibrium moisture content and shrinkage of selected tropical wood species. *BioResources* **2017**, *12*, 597–607.
30. Sjökvist, T.; Niklewski, J.; Blom, A. Effect of wood density and cracks on the moisture content of coated Norway spruce (Picea abies (L.) Karst.). *Wood Fiber Sci.* **2019**, *51*, 160–172.
31. Kojima, M.; Yamamoto, H.; Yoshida, M.; Ojio, Y.; Okumura, K. Maturation

property of fast-growing hardwood plantation species: A view of fiber length. *For. Ecol. Manage.* **2009**, *257*, 15–22.

**7. List of publications**

1. Viet, D.D.; Ma, T.; Inagaki, T.; Kim, N.T.; Chi, N.Q.; Tsuchikawa, S. Physical and mechanical properties of fast growing polyploid acacia hybrids (A. auriculiformis x A. mangium) from Vietnam. *Forests* **2020**, *11*, 1–15.

2. Viet, D.D.; Ma, T.; Inagaki, T.; Kim, N.T.; Tsuchikawa, S. Near-infrared spectroscopy and hyperspectral imaging can aid in the prediction and mapping of polyploid acacia hybrid wood properties in tree improvement programs. Holzforschung (accepted)

In submission: Identification *Acacia* hybrid wood using Near-infrared hyperspectral imaging and deep learning method.

**8. List of Conferences**

Oral Presentation

1. The 36th NIR Forum of the JCNIRS (Japan Council for Near Infrared Spectroscopy). November 2020. Online meeting. Near Infrared spectroscopy and Hyperspectral imaging research for genetic improvement of fast growing polyploid acacia hybrid wood.

2. The 71st Annual Meeting of the JWRS (Japan Wood Research Society). March 2021. Online meeting. Comparison between Near Infrared spectroscopy and Hyperspectral imaging for prediction polyploid acacia hybrid wood properties and mapping wood properties in tree improvement program.

3. Tentative conference: The 20$^{th}$ International Conference on NIR, October 2021. Beijing, China.

**9. Activities**

As of a PhD student in Asia Advanced Agriculture and Data science program (AAAD program) I have studied R and Python program by Data science class. I earned 2 credits from this class and have gotten such a wonderful knowledge in analysis data. It will help me very much in my career.